Chemical Physics 351 (2008) 72–76

Contents lists available at ScienceDirect

Chemical Physics

journal homepage: www.elsevier.com/locate/chemphys

Hydrogen adsorption strength and sites in the metal organic framework MOF5: Comparing experiment and model calculations

F.M. Mulder [a,*], T.J. Dingemans [b], H.G. Schimmel [a], A.J. Ramirez-Cuesta [c], G.J. Kearley [d]

[a] Department of Radiation, Radionuclides and Reactors, Faculty of Applied Sciences, Delft University of Technology, Mekelweg 15, 2629JB Delft, The Netherlands
[b] Faculty of Aerospace Engineering, Delft University of Technology, Kluyverweg 1, 2629 HS Delft, The Netherlands
[c] ISIS Facility, Rutherford Appleton Laboratory, Chilton, Didcot, Oxon OX11 0QX, UK
[d] Bragg Institute, Building 87, Australian Nuclear Science and Technology Organisation, PMB 1 Menai, NSW 2234, Australia

ARTICLE INFO

Article history:
Received 3 December 2007
Accepted 31 March 2008
Available online 7 April 2008

Keywords:
Hydrogen storage
Metal organic framework
Neutron spectroscopy
Adsorption interaction
First principles modelling
MOF5
IRMOF-1

ABSTRACT

Hydrogen adsorption in porous, high surface area, and stable metal organic frameworks (MOF's) appears a novel route towards hydrogen storage materials [N.L. Rosi, J. Eckert, M. Eddaoudi, D.T. Vodak, J. Kim, M. O'Keeffe, O.M. Yaghi, Science 300 (2003) 1127; J.L.C. Rowsell, A.R. Millward, K. Sung Park, O.M. Yaghi, J. Am. Chem. Soc. 126 (2004) 5666; G. Ferey, M. Latroche, C. Serre, F. Millange, T. Loiseau, A. Percheron-Guegan, Chem. Commun. (2003) 2976; T. Loiseau, C. Serre, C. Huguenard, G. Fink, F. Taulelle, M. Henry, T. Bataille, G. Férey, Chem. Eur. J. 10 (2004) 1373]. A prerequisite for such materials is sufficient adsorption interaction strength for hydrogen adsorbed on the adsorption sites of the material because this facilitates successful operation under moderate temperature and pressure conditions. Here we report detailed information on the geometry of the hydrogen adsorption sites, based on the analysis of inelastic neutron spectroscopy (INS). The adsorption energies for the metal organic framework MOF5 equal about 800 K for part of the different sites, which is significantly higher than for nanoporous carbon materials (~550 K) [H.G. Schimmel, G.J. Kearley, M.G. Nijkamp, C.T. Visser, K.P. de Jong, F.M. Mulder, Chem. Eur. J. 9 (2003) 4764], and is in agreement with what is found in first principles calculations [T. Sagara, J. Klassen, E. Ganz, J. Chem. Phys. 121 (2004) 12543; F.M. Mulder, T.J. Dingemans, M. Wagemaker, G.J. Kearley, Chem. Phys. 317 (2005) 113]. Assignments of the INS spectra is realized using comparison with independently published model calculations [F.M. Mulder, T.J. Dingemans, M. Wagemaker, G.J. Kearley, Chem. Phys. 317 (2005) 113] and structural data [T. Yildirim, M.R. Hartman, Phys. Rev. Lett. 95 (2005) 215504].

1. Introduction

Hydrogen adsorption in MOFs has the characteristic of an adsorption interaction which is much lower than the enthalpies of formation of many light metal hydrides. In principle there is an advantage to this low adsorption interaction because this opens the possibility to have rapid hydrogen adsorption into MOFs without running into the limitations of adsorption heat transport out of the storage material, which is a remaining bottleneck with for instance catalysed and nanostructured MgH_2 [8]. However, the disadvantage of the currently found adsorption interactions is that they are still that low that significant storage only occurs at low temperatures or exceedingly high pressures [1–3,9], and therefore the aim is to chemically tailor MOFs to realize higher adsorption energies using various approaches [9–12]. Experimental characterisation of the adsorption potential of hydrogen molecules can be performed using neutron inelastic spectroscopy (INS) [1,13]. Such experiments give detailed information on the local shape of the adsorption potential via the barrier for rotation of the exited $J = 1$ molecular state of H_2, and via the information on the 1, 2 or 3D dimensionality of the rotor [14–16]. Advantages of neutron scattering are its high sensitivity to para hydrogen and the fact that, unlike in optical methods, there are no forbidden transitions or extinction effects that play a role [17].

Modelling of the adsorption interaction in a few types of MOF has been performed by classical methods using force fields in several occasions [18–22], and by using full ab initio methods at the MP2 [23] level for certain fragments of the MOF [5,17,24]. Ab initio calculations using density functional theory were performed in [6,25] on the full primitive cell of MOF5, i.e. on a full periodic model. It may be noted that the adsorption energy values in the DFT results compare favourably with MP2 level calculations [6,24]. In [6] the preferred adsorption sites and also the barriers for rotational tunnelling of the hydrogen molecule were calculated, and for this reason the experimental INS data are compared to these calculations. Additionally, the positions of the adsorption sites in MOF5 have been determined by Yildirim and Hartman in neutron diffraction experiments on deuterated materials. Therefore, the existing experimental information on positions [7] and the here reported

* Corresponding author. Tel.: +31 15 2784870; fax: +31 15 2783803.
E-mail address: f.m.mulder@tudelft.nl (F.M. Mulder).

0301-0104/$ - see front matter © 2008 Elsevier B.V. All rights reserved.
doi:10.1016/j.chemphys.2008.03.034

INS data on the adsorption potentials is compared in this contribution to the theoretical predictions of ab initio calculations on the full periodic structure of [6]. The INS spectroscopic information revealed here and the comparison with existing structural data and modelling results gives new insight in the adsorption potentials experienced by molecular hydrogen in MOF5. Such insight can be used for further optimisation of MOF structures towards higher absorption strength MOFs with high storage capacity.

2. Methods

MOF5 was prepared using a similar method as described in [26]. Samples were stored under a dry and inert atmosphere, in order to prevent possible degradation as reported in [27]. Cubic crystals as grown from the solution ranged in size up to ~0.5 mm. It was noted that the diffraction linewidth increases upon the uptake of possibly water from the air, which may show that strains build up upon adsorption. The composition of the sample was verified using X-ray diffraction on clean and degassed MOF5 sample under an inert atmosphere. Using GSAS [28] the structure was refined having a space group F m-3m with lattice parameter $a = 25.83$ Å.

The adsorption energy of the hydrogen molecules can be obtained from macroscopic adsorption measurements. Experiments were performed using a closed cycle cryostat with a base temperature of 3.6 K. First the sample was loaded in the sample container made of aluminium with a gold O-ring, and degassed at elevated temperature (150 °C) for prolonged periods of time (days) under high vacuum (down to 10^{-4} Pa). After cooling to 60 K hydrogen was loaded in the sample using hydrogen gas that was additionally purified by leading it through a bed of zeolite spheres at 77 K. The amount of hydrogen loaded was determined volumetrically from the pressure drop in a calibrated volume at room temperature. A small correction was made for the free volume of the capillary and the empty sample chamber minus the volume of the sample calculated from the density and weight of the MOF5 sample, and taking into account the sample chamber temperature.

INS was performed using the TOSCA instrument at ISIS (Rutherford Appleton Laboratories, Oxfordshire, UK). Neutrons are predominantly scattered by the protons in the sample because of their large incoherent scattering cross section. Inelastic neutron scattering probes the motions of these hydrogen atoms, i.e. their vibrations (the MOF5 matrix protons) and rotations (the molecular hydrogen). The sample was again loaded in an Al container with a gold O-ring seal and degassed under high vacuum (10^{-4} Pa) at 150 °C. The empty sample was measured at 13 K. After heating to 60 K, calibrated amounts of para hydrogen were loaded in the sample using para hydrogen produced in a separate cryostat. The amounts of para hydrogen loaded were determined from the pressure drop in a known volume at room temperature.

Mulder et al. [6] performed first principles model calculations using density functional theory (DFT) in the generalized gradient approximation (GGA) as implemented in the VASP plane wave pseudo-potential code. Generally DFT codes have limitations in reproducing long-range dispersive interactions like the long-range tails of van der Waals interactions (see, e.g., [29] for a discussion). Recently, however, it was shown that DFT with GGA pseudo potentials give good agreement of the adsorption energy with experimental results for hydrogen adsorbed on carbon [30] and for alkanes adsorbed in zeolites [31]. The rotational barrier that has to be overcome when rotating a H_2 molecule in the calculations as described in [6] is compared to the para to ortho hydrogen rotational transitions observed in the INS. Such DFT methods to reveal the potential energy surface are also employed in for instance understanding the methyl group rotational tunnelling in solids [32].

3. Results and discussion

The hydrogen gas pressure above the sample as a function of temperature is shown in Fig. 1a for a few fixed loadings. For a low amount of hydrogen loaded the adsorbed hydrogen starts to be released partially from MOF5 above 60–70 K, while for increased loading such release already starts at 20–40 K. As described in [4] such data can be fitted to the following equation, which relates the adsorption energy H_{ad}, the site coverage θ, the temperature T and pressure P:

$$P = C'\sqrt{T}\exp\left(-\frac{H_{ad}}{k_B T}\right)\frac{\theta}{1-\theta} \quad (1)$$

where C' is a constant. For the fit one assumes a constant θ, i.e. the free volume of the empty space in the filled sample container should be small. The resulting effective adsorption energies are plotted in Fig. 1b. The value for low hydrogen loadings is remarkable high ~720 to ~850 K. Such values exceed those found in nanostructured carbon materials like nanotubes and activated carbons (~550 K) by up to 54%. Such finding agrees with the first principles calculations reported in [5,6]. This finding indicates that there is considerable promise for the increase of hydrogen adsorption energies by using MOF's and tailoring the substrate.

Adsorption isotherms were measured at three different low temperatures in order to determine the adsorption capacities of stronger as well as weaker bound sites (Fig. 2). Note that the pressures applied are all below the vapour pressure of pure hydrogen (3.24 Bar at 25 K), i.e. no liquid can be formed yet in the free volume between the MOF crystallites. It is immediately obvious from

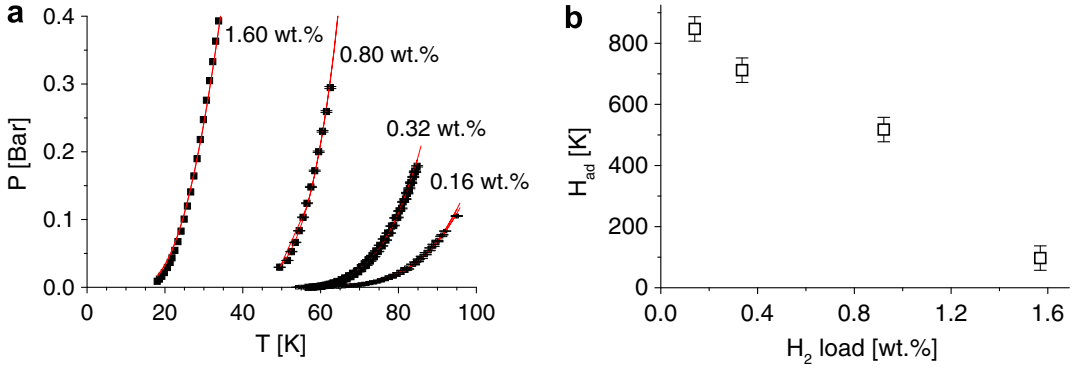

Fig. 1. (a) Hydrogen gas pressure above a sample of MOF5 loaded to the amounts as indicated. The lines are fits giving the effective adsorption energy of the sites that release their hydrogen. (b) The resulting effective adsorption energies as a function of hydrogen loading. Note the relatively high effective adsorption energies up to ~0.3 wt%. A rapid decrease of the effective adsorption energy with increasing loading is observed.

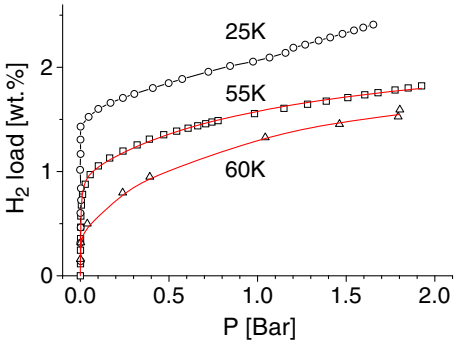

Fig. 2. The hydrogen load as a function of applied pressure at three different temperatures. The 55 and 60 K curves are fitted using two Langmuir isotherms. The steep initial increase represents the stronger bound H_2, while the sloping increase represents the weaker bound H_2.

the measurements that a large fraction of the hydrogen is bound directly at low pressure. Upon increasing the pressure there still is an increasing adsorption, leading to a shape of the isotherms as described in [33] for a system with heterogeneous sites, having different adsorption interaction strengths. The gradual increase of adsorption with pressure occurs mainly because sites with lower adsorption energies become increasingly occupied. Upon lowering the temperature the isotherms change significantly due to the increasingly higher adsorption at less favourable sites. For 55 and 60 K it was possible to fit the data with the sum of only two Langmuir isotherms ($\theta = bP/(1+bP)$ as follows from Eq. (1), where b is a constant), one corresponding to the rapid increase of adsorption, and the second to the gradual increase at increasing pressure. At 25 K two isotherms were not enough to get a reasonable fit, and there is also an indication of a small step at 1.2 Bar. Such findings may be explained by the ordering of hydrogen molecules on the different sites as the coverage of the sites increases at low temperature. Steps in the isotherm for adsorption of methanol in a metal organic framework were observed by Fletcher et al. [34]. In addition, the relatively large mobility of hydrogen between different adsorption sites at temperatures above ~38 K following from molecular dynamics simulations [6] may play a role.

An estimate of the amount of hydrogen adsorbed in these MOF5 crystals with an adsorption energy larger than that in liquid hydrogen can be obtained from extrapolating the 25 K data to 3.24 Bar, the hydrogen vapour pressure at 25 K. This number equals about 3.2 wt%. Above this loading liquid hydrogen will be formed between the crystallites, and if space still permits, inside the MOF5 pores. The adsorption capacity at 60 K is similar to what has been reported by others at 77 K and higher pressures [2,27].

In [6] the adsorption energy was calculated and as stated above the value agrees well with the values found here for low hydrogen loadings, i.e. when only the most preferable sites are occupied. In [6] also predictions for the rotational barriers of adsorbed hydrogen molecules were given which are in principle smaller interactions than the adsorption interaction itself. In order to observe the shape of the potential well experienced by the molecular hydrogen via the rotational transitions, and to be able to compare experimental and computational results, inelastic neutron spectroscopy (INS) was performed. For this comparison also the neutron diffraction results for low deuterium loading of Yildirim and Hartman is used, showing the different deuterium adsorption sites experimentally in MOF5 [7]. In Fig. 3 the data are plotted before and after subtraction of the signal of the empty sample, measured at 13 K. The large increase of the signal with loading of hydrogen is consistent with the amount of hydrogen loaded.

The empty MOF5 sample shows the characteristic vibrations of the BDC (=1,4-benzenedicarboxylate) organic spacer. When hydrogen is loaded, the broad background signal increases, and most important, several new peaks occur at low energy transfers (<20 meV). The broad background is due to recoil of the hydrogen molecule. The narrow peaks correspond to the rotational $J = 0$ to $J = 1$ transition of the H_2 molecule, $J\,(1 \leftarrow 0)$. In principle three lines

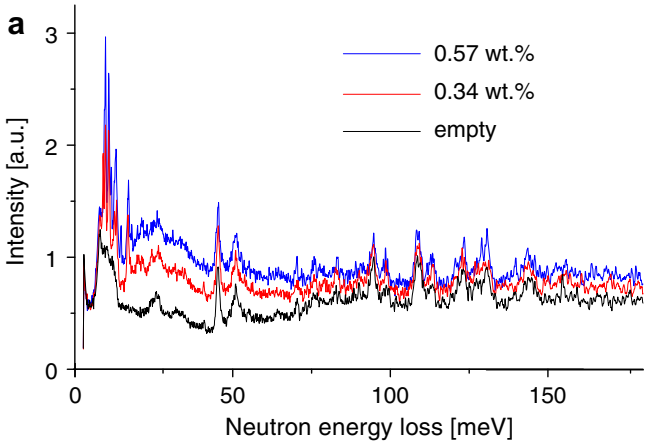

Fig. 3a. INS spectra from MOF5 without and with two different loadings of hydrogen. The peaks between 300 and 1500 cm^{-1} result mainly from modes within the BDC linker. Upon hydrogen loading the general spectrum intensity is lifted due to scattering by the hydrogen (recoil signal). At low energy strong peaks occur that are different rotational transitions of the para H_2 molecules.

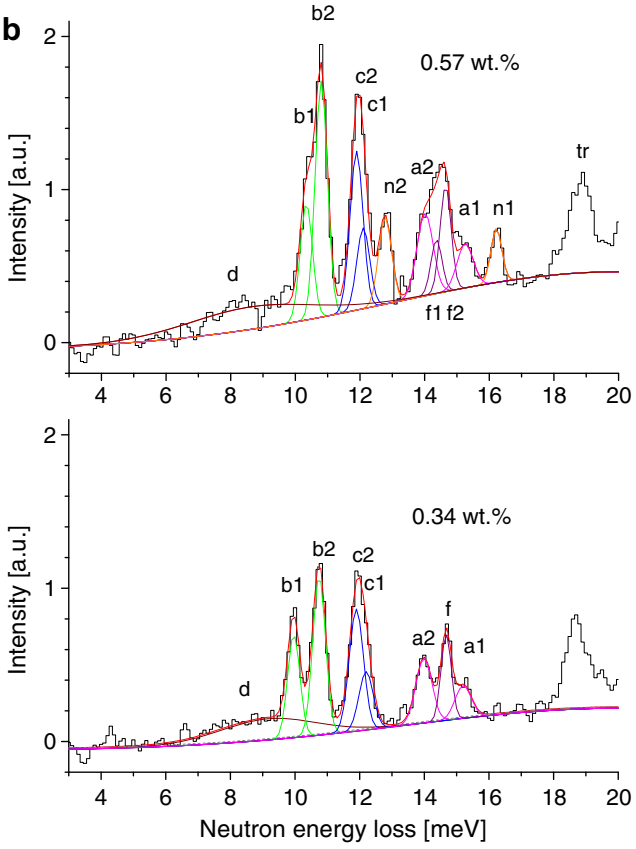

Fig. 3b. The low energy part of the spectra after subtraction of the empty MOF5 signal for the two different loadings (1 meV = 8.066 cm^{-1}). Peaks are rotational transitions of the adsorbed hydrogen molecules. Fits that indicate up to five different sites for H_2 are presented, with the colours indicating different sub-spectra (i.e. molecular sites). Note that for the higher loading apart from larger intensities, new peaks $n1$,$n2$ and a peak shift ($b1$) occur.

are present (initial $m = 0$, final $m = -1, 0, +1$) of which the degeneracy is lifted depending on the geometry of the site in which hydrogen is adsorbed. For hydrogen in pure solid hydrogen the environment is isotropic and a single threefold degenerate transition at 14.7 meV occurs. For adsorption on surfaces or in strongly hindered sites the degeneracy can be lifted, which thus gives information on the number of different sites and their geometry. The fitting of the spectra is performed using constraints on the intensities of the sub-spectra peaks as should be the case for rotational transitions $(J,m) = (0,0)$ to $(J,m) = (1,0)$, or J,m $(1,0 \leftarrow 0,0)$ and $(J,m) = (0,0)$ to $(J,m) = (1,\pm1)$, or J,m $(1,\pm1 \leftarrow 0,0)$ (peak intensities should have ratio 1:2). The widths for peaks belonging to one sub-spectrum are constrained to be about the same. The two different loadings measured give additional handles on which peaks contribute to the same sub-spectrum. The resulting fits are shown in Fig. 3, and the parameters are in Table 1. The good resolution of the spectra allows the discrimination of up to five different contributing sub-spectra and one broad diffuse contribution, which could not be achieved in the work of [1].

The spectra show large splittings and also shifts of the centre of mass compared to the 14.7 meV peak position of solid hydrogen. This clearly indicates that most adsorption sites are far from isotropic, and that there is significant interaction with the substrate. The barriers for molecular rotation can be obtained using the standard anisotropic potential of the form $V(\theta) = V_0 \cdot \cos^2(\theta)$, where V_0 is the potential energy barrier height. For positive values of the parameter V_0 the molecule aligns parallel to a surface (2D case) and for negative values of V_0 the molecules is perpendicular to a surface (1D case). In the 2D case the degeneracy on the quantum number $m = \pm1$, means that the lower energy peak will have twice the intensity of the higher energy component, whereas in the 1D case the opposite is true. Using the model described in [14] we can estimate a barrier height as well as an apparent rotational constant for the hindered hydrogen rotor expressed in units b_{H_2}, which is the rotational constant for unperturbed H_2 (last 2 columns in Table 1). The origin of the diffuse contribution indicated by d may be found in adsorbed hydrogen molecules that follow the modes of the MOF matrix that are relatively strong in this area; then it is not related to rotational transitions.

In [6] first principles calculations are described to determine potential favourable adsorption sites for H_2. The results indicated at least four different positions with relatively high adsorption energies, as is found here experimentally in the lowest loading. Low adsorption energy sites were not considered in these calculations. When comparing the calculated favourable positions of [6] with the neutron diffraction experiments of [7] we can see that there is good agreement: the positions of the C_6, Zn-wide, Zn-narrow, sites of [6] correspond with, respectively, the Hex, Cup, and ZnO_3 site of [7]. Only the O–CO_2 appears to be shifted from the ZnO_2 site (see below). In order to assign the sub-spectra of Table 1 to these different sites we can use the multiplicity of these sites in [7] which would be expected to scale in a first approximation with the intensity of the sub-spectra. These multiplicities are 48, 32, 32, 96 for, respectively, the C_6/Hex, Zn-wide/Cup, Zn-narrow/ZnO_3 and O–CO_2/ZnO_2 sites. In addition, in [6] the barrier for rotation was calculated for the sites, and these barriers can now be compared with the INS experimental values in Table 1. Comparing the intensity and barriers measured with the multiplicity and the barriers calculated in [6] one arrives at the spectral assignments of the $b_{1,2}$, $c_{1,2}$, $a_{1,2}$ and $f_{1,2}$ to, respectively, the O–CO_2/ZnO_2, C_6/Hex, Zn-wide/Cup, and Zn-narrow/ZnO_3 sites. With this assignment the calculated barriers appear to follow the measured ones (see Table 1) although the Zn-wide site has the highest experimental barrier (6 meV) but still lower than the calculated one (10–13 meV). As stated above the O–CO_2 site calculated in [6] is shifted from the experimental ZnO_2 site [7]. In addition, for the higher loading measured here we see the peaks of this site shift in position. In [6] the model calculations were performed on a system where the sites were only partly occupied in order to determine possible preferential adsorption sites. It was mentioned that when all sites would be occupied simultaneously there would be significant interference of these sites. Therefore, the shifting positions of the $b_{1,2}$ lines may indicate just this interference where the ZnO_2 site is representative of the hydrogen system with higher filling. The position of the O–CO_2 site is such that it will interfere most with the Zn-narrow/ZnO_3 site. In the spectra of Figs. 3a and 3b and in Table 1 there is indeed also a slight change in the peak positions $f_{1,2}$ (splitting) upon increased loading.

Table 1
Parameters for the observed peak positions at para hydrogen loading of 0.34 and 0.57 wt%, respectively

Peaks @ 0.34 wt%	Position (meV)	Intensity (a.u.)	1D or 2D	Width (meV)	Rotation barrier (meV)	Apparent rotational constant (b_{H_2})	Assignment, multiplicity of [12], calculated barrier (meV) of [6]
D	9.2	0.5		3			
*b*1,*b*2	9.96, 10.75	0.32, 0.51	1D	0.38, 0.39	3.94	0.71	O–CO_2 96 2–5
*c*2,*c*1	11.90, 12.20	0.44, 0.21	2D	0.44, 0.44	1.49	0.82	C_6 48 0–3
*a*2,*a*1	13.99, 15.20	0.26, 0.13	2D	0.50, 0.50	6.04	0.98	Zn-wide 32 10–13
f	14.67	0.22	3D	0.32	0	0.98	Zn-narrow 32 0–1
*n*2,*n*1	–	–		–			

Peaks @ 0.57 wt%	Positions (meV)	Intensity (a.u.)	1D/2D	Widths (meV)	Rotational barrier (meV)	Apparent rotational constant (b_{H_2})
D	8.6	0.7		4		
*b*1,*b*2	10.34, 10.80	0.36, 0.74	1D	0.38, 0.38	2.30	0.72
*c*2,*c*1	11.89, 12.10	0.52, 0.26	2D	0.40, 0.40	1.05	0.81
*a*2,*a*1	14.01, 15.25	0.34, 0.18	2D	0.50, 0.50	6.2	0.98
*f*1,*f*2	14.37, 14.65	0.15, 0.29	2D	0.34, 0.34	1.39	0.98
*n*2,*n*1	12.77, 16.22	0.29, 0.15	2D	0.40, 0.34	17.3	0.94

The error in the peak positions is about 0.03 meV. Peaks *x*1, *x*2 assigned to the same sub-spectrum have intensity ratio close to 1:2, and have the same widths. The rotational barrier heights have been calculated according to the standard anisotropic model [16].

For the highest loading measured in this work a new doublet contribution $n1$,$n2$ centred around 14.4 meV is present. Such signal is interpreted as hydrogen molecules on sites that are less preferred than the sites occupied for lower loadings, and may therefore be thought of as a second layer of hydrogen molecules on top of the first molecules adsorbed in the pores. Although not being a preferable site, the barrier for rotation is the highest measured (17.3 meV). In [7] there are also additional sites indicated inside the free space of the pores.

The barrier for rotation and the dimensionality indicated in Table 1 present a description of the potential experienced by the hydrogen molecules at the sites indicated. The experimental results obtained here for the rotational barrier and the sites located by [7] for low hydrogen loadings compare remarkably well with the model calculations in [6]. Also the adsorption interaction strength from the adsorption measurements at low loadings in Fig. 1b ($\sim$700 K) compares well with that of the four preferable sites in [6] (66–72 meV).

4. Conclusions

Summarizing, the adsorption of hydrogen in MOF5 occurs on up to five different adsorption sites, as is observed from neutron inelastic spectroscopy. The combination of structure results from [7], modelling in [6] and the present INS results facilitates the assignment of the INS sub-spectra to specific crystallographic adsorption sites. The neutron inelastic spectroscopy shows that the hydrogen molecules on different sites influence each other upon increasing loading. The adsorption energy for these different sites ranges between 800 and 100 K for, respectively, strongly and more weakly bound sites. The high adsorption energy compares favourably with what is found in nanostructured carbon materials, i.e. there appears potential for improving adsorption energies by application of chemically tailored MOFs. The combined results may indicate that the model calculations can be used remarkably successfully in this type of metal organic frameworks for predicting adsorption sites, and hydrogen–matrix interactions, where also more subtle parameters as the barriers for rotation are predicted well.

Acknowledgements

This work is part of the Delft Institute for Sustainable Energy (DISE) and the Delft Centre for Materials (DCMat). Financial support was received from the Dutch Science Foundation (NWO) for access to ISIS. We thank Dr. S.F. Parker for his support during the experiments at ISIS.

References

[1] N.L. Rosi, J. Eckert, M. Eddaoudi, D.T. Vodak, J. Kim, M. O'Keeffe, O.M. Yaghi, Science. 300 (2003) 1127.
[2] J.L.C. Rowsell, A.R. Millward, K. Sung Park, O.M. Yaghi, J. Am. Chem. Soc. 126 (2004) 5666.
[3] G. Ferey, M. Latroche, C. Serre, F. Millange, T. Loiseau, A. Percheron-Guegan, Chem. Commun. (2003) 2976;
T. Loiseau, C. Serre, C. Huguenard, G. Fink, F. Taulelle, M. Henry, T. Bataille, G. Férey, Chem. Eur. J. 10 (2004) 1373.
[4] H.G. Schimmel, G.J. Kearley, M.G. Nijkamp, C.T. Visser, K.P. de Jong, F.M. Mulder, Chem. Eur. J. 9 (2003) 4764.
[5] T. Sagara, J. Klassen, E. Ganz, J. Chem. Phys. 121 (2004) 12543.
[6] F.M. Mulder, T.J. Dingemans, M. Wagemaker, G.J. Kearley, Chem. Phys. 317 (2005) 113.
[7] T. Yildirim, M.R. Hartman, Phys. Rev. Lett. 95 (2005) 215504.
[8] H.G. Schimmel, J. Am. Chem. Soc. 127 (2005) 14348.
[9] G. Ferey, Chem. Soc. Rev. 37 (2008) 191.
[10] J.L.C. Rowsell, O.M. Yaghi, J. Am. Chem. Soc. 128 (2006) 1304.
[11] M. Dinca, J.R. Long, J. Am. Chem. Soc. 129 (2007) 11172.
[12] S.Q. Ma, H.C. Zhou, J. Am. Chem. Soc. 128 (2006) 11734.
[13] Y. Liu et al., J. Alloy Comp. 446 (2007) 385.
[14] P.C.H. Mitchell, S.F. Parker, A.J. Ramirez-Cuesta, J. Tomkinson, Vibrational Spectroscopy with Neutrons: with Applications in Chemistry, Materials Science and Catalysis, World Scientific, 2005, ISBN 981-256-013-0;
A.J. Ramirez-Cuesta, P.C.H. Mitchell, S.F. Parker, J. Mol. Catal. A 167 (2001) 217.
[15] A.J. Ramirez-Cuesta, P.C.H. Mitchell, Catal. Today 120 (2007) 368.
[16] H.G. Schimmel, G.J. Kearley, F.M. Mulder, Chem. Phys. Chem. 5 (2004) 1053.
[17] S. Bordiga et al., J. Phys. Chem. B 109 (2005) 18237.
[18] L. Sarkisov, T. Duren, R.Q. Snurr, Mol. Phys. 102 (2004) 211.
[19] D. Dubbeldam et al., Fluid Phase Equilibria 261 (2007) 152.
[20] J.L. Belof et al., J. Am. Chem. Soc. 129 (2007) 15202.
[21] M. Tafipolsky, S. Amirjalayer, R. Schmid, J. Comput. Chem. 28 (2007) 1169.
[22] Q.Y. Yang, C.L. Zhong, J. Phys. Chem. B 110 (2006) 655.
[23] C. Møller, M.S. Plesset, Phys. Rev. 46 (1934) 618.
[24] F. Negri, N. Saendig, Theoretical Chem. Accounts 118 (2007) 149.
[25] T. Mueller, G. Ceder, J. Phys. Chem. B 109 (2005) 17974.
[26] M. Eddaoudi, D.B. Moler, H. Li, B. Chen, T.M. Reineke, M. O'Keeffe, O.M. Yaghi, Acc. Chem. Res. 34 (2001) 319.
[27] B. Panella, M. Hirscher, Adv. Mater. 17 (2005) 538.
[28] A.C. Larson, R.B. Von Dreele, General structure analysis system (GSAS), Los Alamos National Laboratory Report LAUR 86-748, 2000.
[29] S. Grimme, J. Comput. Chem. 25 (2004) 1463.
[30] H.G. Schimmel, M.G. Nijkamp, G.J. Kearley, A. Rivera, K.P. de Jong, F.M. Mulder, J. Mater. Sci. Eng. B 108 (2004) 124.
[31] L. Benco, T. Demuth, J. Hafner, F. Hutschka, H. Toulhoat, J. Chem. Phys. 114 (2001) 8.
[32] M. Plazanet, M.R. Johnson, H.P. Trommsdorff, Opt. Spec. 98 (2005) 692.
[33] J.H. de Boer, The Dynamical Character of Asdsorption, Clarendon Press, Oxford, 1968.
[34] A.J. Fletcher, E.J. Cussen, T.J. Prior, M.J. Rosseinsky, C.J. Kepert, K.M. Thomas, J. Am. Chem. Soc. 123 (2001) 10001.